# Supporting Information

## Multifunctional drug carrier on basis of 3d-4f Fe/La-MOFs for drug delivery and dual-mode imaging

Caixue Lin[a‡], Bin Chi[b‡], Chen Xu[a‡], Cheng Zhang[c‡], Feng Tian[a], Zushun Xu[a], Ling Li[a]*, Andrew K. Whittaker[c]*, Jing Wang[b]*

[a.] Ministry-of-Education Key Laboratory for the Synthesis and Application of Organic Function Molecules, Hubei Collaborative Innovation Center for Advanced Organic Chemical Materials, Hubei University 430062, People's Republic of China.

[b.] Australian Institute for Bioengineering and Nanotechnology, ARC Centre of Excellence in Convergent Bio-Nano Science and Technology, The University of Queensland, Brisbane Qld 4072

[c.] Department of Radiology, Union Hospital, Tongji Medical College, Huazhong University of Science and Technology, Wuhan 430022, China

## Contents

**Table S1.** Reports on materials for dual mode imaging.

| Materials | Imaging | Ref |
|---|---|---|
| Porphyrins | MRI/FOI | 1 |
| Gd-/Eu-chelate | MRI/FOI | 2 |
| Gadolinium(III)-coumarin | MRI/FOI | 3 |
| $(Mn_xFe_{1-x})Fe_2O_4/SiO_2$ | MRI/FOI | 4 |
| FA-PEI-$NaGdF_4$:Eu | MRI/FOI | 5 |
| Gadolinium(III) – fluorescein | MRI/FOI | 6 |
| GdNGs | MRI/FOI | 7 |
| $DySiO_2$ – $(Fe_3O_4)_n$ nanoparticles | MRI/FOI | 8 |
| Gold nanorod/$Fe_3O_4$ nanoparticle | MRI/FOI | 9 |
| Upconversion core/porous silica shell nanotheranostics | Magnetic/Luminescent | 10 |
| Folic acid-conjugated Silica-modified gold nanorods | X-ray/CT imaging | 11 |
| First molecular rotor (RY3) | Ratiometry imaging /Fluorescence lifetime imaging | 12 |
| Gd-Au DENPs | CT/MR imaging | 13 |
| ICG-loaded Au@$SiO_2$ | X-ray/CT | 14 |
| Multifunctional polymer microbubbles | Ultrasound/Magnetic resonance imaging | 15 |
| UCNPs@MIL-PEG | MRI/FOI | 16 |

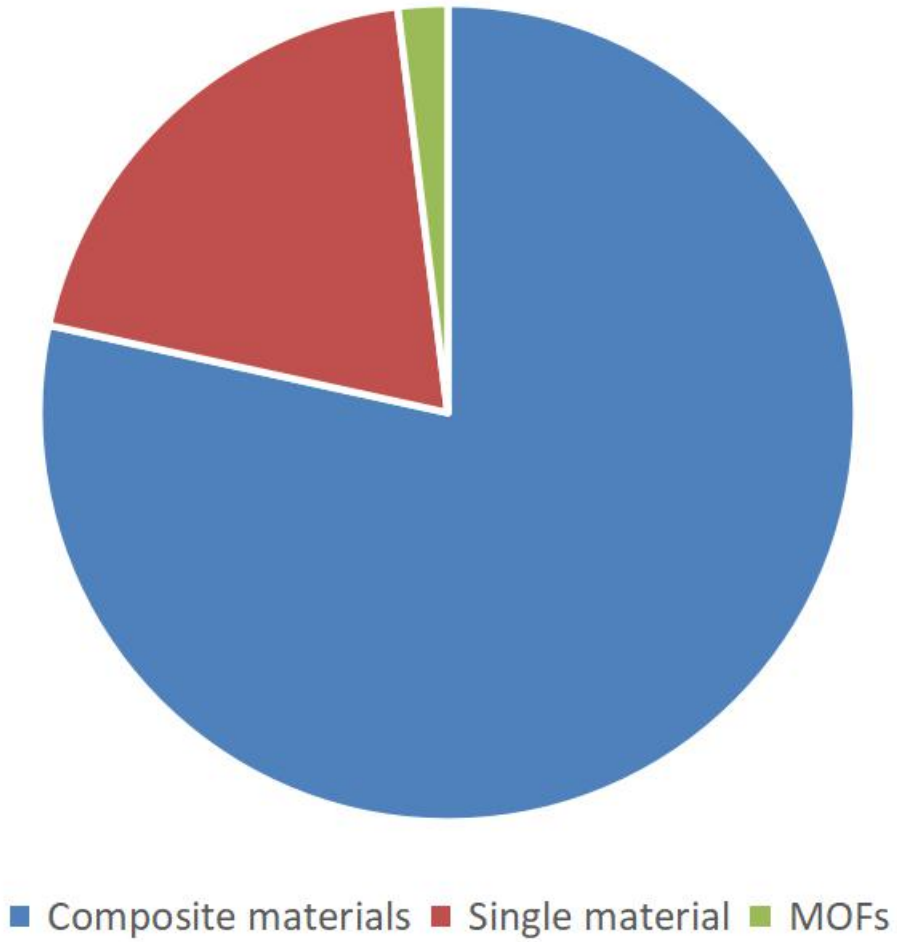


**Figure S1.** Materials for dual mode imaging.

**References:**

[1] X.A. Zhang, K.S. Lovejoy, A. Jasanoff, S.J. Lippard, *P. Natl. Acad. Sci. USA.* **2007,** 104 (26), 10780.

[2] S.G. Crich, L.V. Biancone, D. Duo, G. Esposito, S. Russo, G. Camussi, S. Aime, *Magn. Reson. Med.* **2004,** 51, 938.

[3] Y. Wang, X. Wang, Q. Meng, H. Jia, R. Zhang, P. Zhu, R. Song, H. Feng, Z. Zhang, *Tetrahedron.* **2017,** 73, 38.

[4] Y. Sheng, S. Li, Z. Duan, R. Zhang, J. Xue, *Mater. Chem. Phys.* **2017.**

[5] S. Huang, P. Chen, C. Xu, Facile preparation of rare-earth based fluorescence/MRI dual-modal nanoprobe for targeted cancer cell imaging, *Talanta.* **2017,** 165, 161.

[6] D. Dong, X. Jing, X. Zhang, X. Hu, Y. Wu, C. Duan, *Tetrahedron.* **2012,** 68, 306.

[7] C.K. Lim, A. Singh, J. Heo, D. Kim, K.E. Lee, H. Jeon, J. Koh, I.C. Kwon, S. Kim,

*Biomaterials.* **2013,** 34, 6846.

[8] J.H. Lee, Y.W. Jun, S.I. Yeon, J.S. Shin, J. Cheon, *Angew. Chem.* **2006,** 118, 8340.

[9] C. Wang, J. Chen, T. Talavage, J. Irudayaraj, *Angew. Chem.* **2009,** 121, 2759.

[10] W. Fan, B. Shen, W. Bu, F. Chen, K. Zhao, S. Zhang, L. Zhou, W. Peng, Q. Xiao, H. Xing, *J. Am. Chem. Soc.* **2013,** 135, 6494.

[11] P. Huang, L. Bao, C. Zhang, J. Lin, T. Luo, D. Yang, M. He, Z. Li, G. Gao, B. Gao, *Biomaterials.* **2011,** 32, 9796.

[12] X. Peng, Z. Yang, J. Wang, J. Fan, Y. He, F. Song, B. Wang, S. Sun, J. Qu, J. Qi, *J. Am. Chem. Soc.* **2011,** 133, 6626.

[13] S. Wen, K. Li, H. Cai, Q. Chen, M. Shen, Y. Huang, C. Peng, W. Hou, M. Zhu, G. Zhang, *Biomaterials.* **2013,** 34, 1570.

[14] C. Zhou, D. Cui, G. Shen, G. Gao, P. Huang, Q. Ren, S. Fu, T. Luo, *Opt. Express.* **2011,** 19, 17030.

[15] C. Niu, Z. Wang, G. Lu, T.M. Krupka, Y. Sun, Y. You, W. Song, H. Ran, P. Li, Y. Zheng, *Biomaterials.* **2013,** 34, 2307.

[16] Y.N. Liu, C. Zhang, H. Liu, Y.B. Yi, Z.S. Xu, L. Li, A. Whittaker, *J. Alloy. Compd.* **2018,** 749, 939.

**Table S2.** Reports on 3d-4f heterometallic MOFs.

| Metal ions | Ligand | Application | Ref |
|---|---|---|---|
| $Ni^{2+}$, $Dy^{3+}$ | D-$H_2$Cam | — | 1 |
| $Ln^{3+}$ (Ln=Eu,Gd,Dy,Ho,Er,Tm,Yb,Lu), $Zn^{2+}$ | 4′-(4-carboxyphenyl)−2,2′:6′,2″-terpyridine) | — | 2 |
| $Ln^{3+}$ (Ln=Tb,Dy), $Cu^{2+}$ | iminodiacetate acid | — | 3 |
| $Ln^{3+}$(Ln=Tb,Eu), $Cu^{2+}$ | 2,4′-biphenyldicarboxylic acid | — | 4 |
| $Ln^{3+}$(Ln=Eu,Gd), $Mn^{2+}$ | 5-(isonicotinamido)isophthalic acid | — | 5 |
| $Tm^{3+}$, $Cu^{2+}$ | benzene-1,2-dicarboxylate; isonicotinate | — | 6 |
| $Zn^{2+}$, $Eu^{3+}$ | pyridine-2,5-dicarboxylate; 1,4-benzenedicarboxylate | — | 7 |
| $Ln^{3+}$(Ln=La,Eu,Gd), $Cu^{2+}$ | oxalate； nicotinate | — | 8 |

| | | | |
|---|---|---|---|
| $Ln^{3+}$(Ln=Yb,Ho), $Co^{2+}$ | imidazole-4, 5-dicarboxylic acid | — | 9 |
| $Ln^{3+}$(Ln=Ho,Nd,Sm,Pr), $Cu^{2+}$ | 3-(1H-tetrazol-5-yl)benzoate | — | 10 |
| Pr3+, Cu2+ | isonicotinic acid | — | 11 |
| $Ln^{3+}$(Ln=Eu,Gd,Sm,Tb), $Cu^{2+}$ | pyridine-2,5-dicarboxylic acid | UV-light photocatalytic $H_2$ | 12 |
| $Ln^{3+}$(Ln=Eu,Tb), $Zn^{2+}$ | furan-2,5-dicarboxylic acid | detection of aniline | 13 |
| $Ln^{3+}$(Ln= La, Ce, Pr, Nd and Eu), $Cu^{2+}$ | mesoxalic or dihydroxymalonic acid; dimethylsulfoxide | — | 14 |
| $Ln^{3+}$(Ln=Nd,Ho,Er,Yb), $Zn^{2+}$ | 1H-2-methyl-4,5-imidazole-dicarboxylic acid | — | 15 |
| $La^{3+}$, $Fe^{3+}$ | $H_3BTC$ | fluorescence and MR imaging; drug delivery | This work |

**References:**


[1] X. Tan, Y.Z. Du, Y.X. Che, J.M. Zheng, *Inorganic Chem. Comm.* **2013,** 36, 63.

[2] X. Zhang, C. Chen, X. Liu, P. Gao, M. Hu, *J. Solid. State. Chem.* **2017.**

[3] J.X. Ma, X.F. Huang, X.Q. Song, L.Q. Zhou, W.S. Liu, *Inorg. Chim. Acta.* **2009,** 362, 3274.

[4] X.-Y. Yi, Y. Ying, H.-C. Fang, Z.-G. Gu, S.-R. Zheng, Q.-G. Zhan, L.-S. Jiang, W.-S. Li, F.-Q. Sun, Y.-P. Cai, *Inorg. Chem. Comm.* **2011,** 14, 453.

[5] M.S. Chen, W. Li, C.H. Zhang, D.Z. Kuang, Y.F. Deng, Z.M. Chen, *Inorg. Chim. Acta.* **2012,** 382, 177.

[6] G.M. Wang, J.H. Li, Z.X. Li, P. Wang, Y.X. Wang, J.H. Lin, *Solid. State. Sci.* **2012,** 14, 445.

[7] Y.Y. Bai, Y. Huang, B. Yan, Y.S. Song, L.H. Weng, *Inorg. Chem. Comm.* **2008,** 11, 1030.

[8] G. Peng, Y.C. Qiu, Z.H. Liu, Y.H. Li, B. Liu, H. Deng, *Inorg. Chem. Comm.* **2008,** 11, 1409.

[9] L.C. Zhu, Y. Zhao, S.J. Yu, M.M. Zhao, *Inorg. Chem. Comm.* **2010,** 13, 1299.

[10] L. Li, G. Li, L. Sun, G. Lan, L. Zhang, C. Yang, Y. Ma, H. Deng, *Inorg. Chem. Comm.* **2012,** 20, 295.

[11] H.G. Jin, X.J. Hong, H.C. Tan, W. Qin, X.M. Lin, Y.P. Cai, *Crystengcomm.* **2017.**

[12] X.L. Hu, C.Y. Sun, C. Qin, X.L. Wang, H.N. Wang, E.L. Zhou, W.E. Li, Z.M. Su, *Chem. Commun.* **2013,** 49 (34), 3564.

[13] L. Li, J.Y. Zou, S.Y. You, H.M. Cui, G.P. Zeng, J.Z. Cui, *Dalton. T.* **2017,** 46, 16432.

[14] B. Gilhernández, P. Gili, M. Quirós, J. Sanchiz, *Crystengcomm.* **2015,** 17, 6555.

[15] X. Feng, Y.Q. Feng, J.J. Chen, S.W. Ng, L.Y. Wang, J.Z. Guo, *Dalton. T.* **2014,** 44, 804.

**Table S3.** Reports on pH-responsive release of DOX from silica-containing compounds.

| Materials | DOX release percent (%) | | The difference (%) | Ref |
|---|---|---|---|---|
| | Simulation pH of normal cells | Simulation pH of cancer cells | | |
| DOX-$Cu_9S_5$@m$SiO_2$-PG | 5% | 43% | 38% | 1 |
| $Cu_9S_5$@m$SiO_2$@$Fe_3O_4$-PEG | 0% | 22.5% | 22.5% | 2 |
| DOX-$Fe_3O_4$@m$SiO_2$-PO-FA | 20% | 73% | 53% | 3 |
| $Fe_3O_4$@m$SiO_2$-FA-CuS-PEG | 10% | 50% | 40% | 4 |
| CuS@m$SiO_2$-PEG | 10% | 35% | 25% | 5 |
| Se@$SiO_2$-FA-CuS | 20% | 48% | 28% | 6 |
| PB@m$SiO_2$-PEG/DOX | 3% | 45% | 42% | 7 |
| RGO@m$SiO_2$-DOX/HA | 30% | 60% | 30% | 8 |
| Se@$SiO_2$/DOX | 12% | 92% | 80% | 9 |
| $Fe_3O_4$@$SiO_2$ | 10% | 80% | 70% | 10 |
| $Mn_3[Co(CN)_6]_2$@$SiO_2$@Ag | 35% | 65% | 30% | 11 |
| Au-HMSN | 50% | 90% | 40% | 12 |
| $SiO_2$–ZnO | 60% | 75% | 15% | 13 |
| $Fe_3O_4$–CdTe@$SiO_2$ | 48% | 80% | 32% | 14 |
| β-$NaYF_4$:$Ce^{3+}$/$Tb^{3+}$@m$SiO_2$-PEG | 22% | 65% | 43% | 15 |
| GNR@m$SiO_2$ | 2% | 60% | 58% | 16 |
| Fe/La-MOFs@$SiO_2$-$NH_2$ | 8% | 95% | 87% | This work |

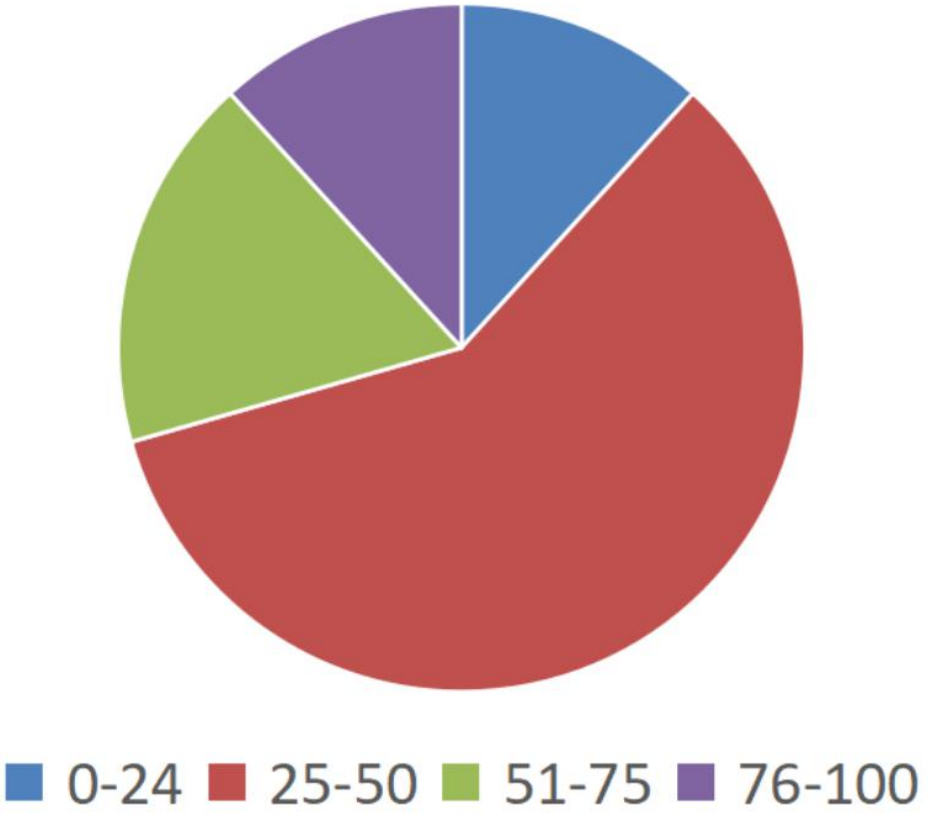


**Figure S2.** Plot of pH-responsive release of DOX from silica-containing compounds

**References:**

[1] Y. Chen, Z. Hou, B. Liu, S. Huang, C. Li, J. Lin, *Dalton. T.* **2015,** 44, 3118.

[2] B. Liu, X. Zhang, C. Li, F. He, Y. Chen, S. Huang, D. Jin, P. Yang, Z. Cheng, J. Lin, *Nanoscale.* **2015,** 8, 12560.

[3] X. Luo, Y. Wang, H. Lin, F. Qu, *Rsc. Adv.* **2016,** 6, 113.

[4] Z. Gao, X. Liu, G. Deng, F. Zhou, L. Zhang, Q. Wang, J. Lu, *Dalton. T.* **2016,** 45, 13456.

[5] X. Liu, Q. Ren, F. Fu, R. Zou, Q. Wang, G. Xin, Z. Xiao, X. Huang, Q. Liu, J. Hu, *Dalton. T.* **2015,** 44, 10343.

[6] Y. Wang, X. Liu, G. Deng, J. Sun, H. Yuan, Q. Li, Q. Wang, J. Lu, *Nanoscale.* **2018**.

[7] Y.Y. Su, W.F. Liu, Y. Liu, G.M. Lu, *Acs. Appl. Mater. Inter.* **2016,** 8, 17038.

[8] Y. Yang, Y. Wang, W. Xu, X. Zhang, Y. Shang, A. Xie, Y. Shen, *Eur. J. Inorg. Chem.* **2017.**

[9] X. Liu, G. Deng, Y. Wang, Q. Wang, Z. Gao, Y. Sun, W. Zhang, J. Lu, J. Hu, *Nanoscale.* **2016,** 8, 8536.

[10] X. Hu, Y. Wang, L. Zhang, M. Xu, J. Zhang, W. Dong, *Chemmedchem.* **2017,** 12, 1600.

[11] D. Wang, Z. Guo, J. Zhou, J. Chen, G. Zhao, R. Chen, M. He, Z. Liu, H. Wang, Q. Chen, *Small.* **2015,** 11, 5956.

[12] G. Chang, Y. Shen, C. Pei, L. Chen, *MATEC Web of Conferences.* **2016,** 01013.

[13] V.B. Kumar, M. Annamanedi, M.D. Prashad, K.M. Arunasree, Y. Mastai, A. Gedanken, P. Paik, *J. Nanopart. Res.* **2013,** 15, 1.

[14] G. Wang, L. Jin, Y. Dong, L. Niu, Y. Liu, F. Ren, X. Su, *New. J. Chem.* **2014,** 38, 700.

[15] Ma, Ping'an, Li, Chunxia, Lin, Jun, Wu, Yang, *Dalton. T.* **2013,** 42, 9852.

**[16]** T. Zhang, Z. Ding, H. Lin, L. Cui, C. Yang, X. Li, H. Niu, N. An, R. Tong, F. Qu, *Eur. J. Inorg. Chem.* **2015,** 2015, 2277.

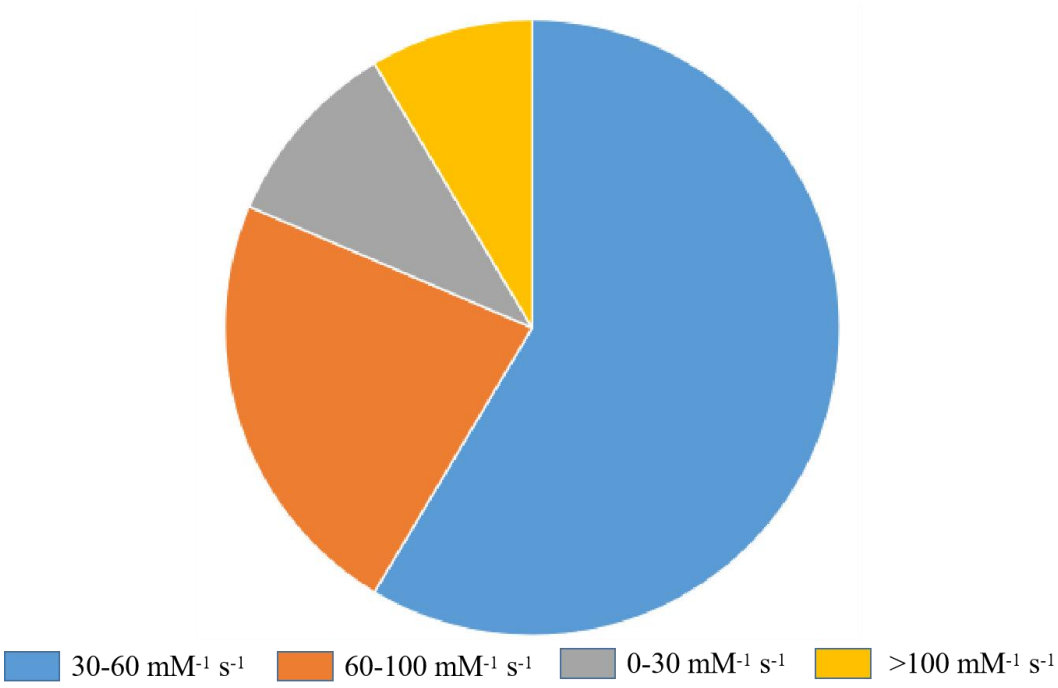


**Figure S3.** $T_2$-weighted MR relaxivity ($r_2$) of other MOFs.

**References:**

[1] D. Wang, J. Zhou, R. Chen, R. Shi, G. Zhao, G. Xia, R. Li, Z. Liu, J. Tian, H. Wang, *Biomaterials.* **2016,** 100, 27.

[2] D. Wang, J. Zhou, R. Shi, H. Wu, R. Chen, B. Duan, G. Xia, P. Xu, H. Wang, S. Zhou, *Theranostics.* **2017,** 7, 4605.

[3] M.A. Chowdhury, *J. Biomed. Mater. Res. A.* **2017,** 105, 1184.

[4] J. Della Rocca, W. Lin, *Eur. J. Inorg. Chem.* **2010,** 24, 3725.

[5] J. Meng, X. Chen, Y. Tian, Z. Li, Q. Zheng, *Chemistry.* **2017,** 23, 69.

[6] W.J. Rieter, K.M. Taylor, H. An, W. Lin, W. Lin, *J. Am. Chem. Soc.* **2006,** 128, 9024.

[7] D. Liu, K. Lu, C. Poon, W. Lin, *norg. Chem.* **2014,** 53, 1916.

[8] W. Zhu, Y. Liu, Z. Yang, L. Zhang, L. Xiao, P. Liu, J. Wang, C. Yi, Z. Xu, J. Ren, *J. Mater. Chem. B.* **2017,** 6, 2.

[9] R.J. Della, D. Liu, W. Lin, *Journal of Shanghai Normal University.* **2012,** 44, 957.

[10] C.A. Ray, D. Bhattacharya, S.K. Sahu, *Dalton. T.* **2016,** 45, 2963.

[11] M.D. Rowe, C.C. Chang, D.H. Thamm, S.L. Kraft, H.J. Jr, A.P. Vogt, B.S. Sumerlin, S.G. Boyes, *Langmuir.* **2009,** 25, 9487.

[12] S.E.H. Murph, S. Jacobs, J. Liu, C.C. Hu, M. Siegfired, S.M. Serkiz, J. Hudson, *J. Nanopart. Res.* **2012,** 14, 1.

[13] L. Han, J. Li, S. Huang, R. Huang, S. Liu, X. Hu, P. Yi, D. Shan, X. Wang, H. Lei, *Biomaterials.* **2011,** 32, 2989.

[14] W. Lin, R.A. Fischer, J.S. Chen, D.E.D. Vos, *Eur. J. Inorg. Chem.* **2010,** 24.

[15] X. Li, Y. Qian, T. Liu, X. Hu, G. Zhang, Y. You, S. Liu, Amphiphilic multiarm star block copolymer-based multifunctional unimolecular micelles for cancer targeted drug delivery and MR imaging, *Biomaterials.* **2011,** 32, 6595.

[16] S. Baek, R.K. Singh, D. Khanal, K.D. Patel, E.J. Lee, K.W. Leong, W. Chrzanowski, H.W. Kim, *Nanoscale.* **2015,** 7, 14191.

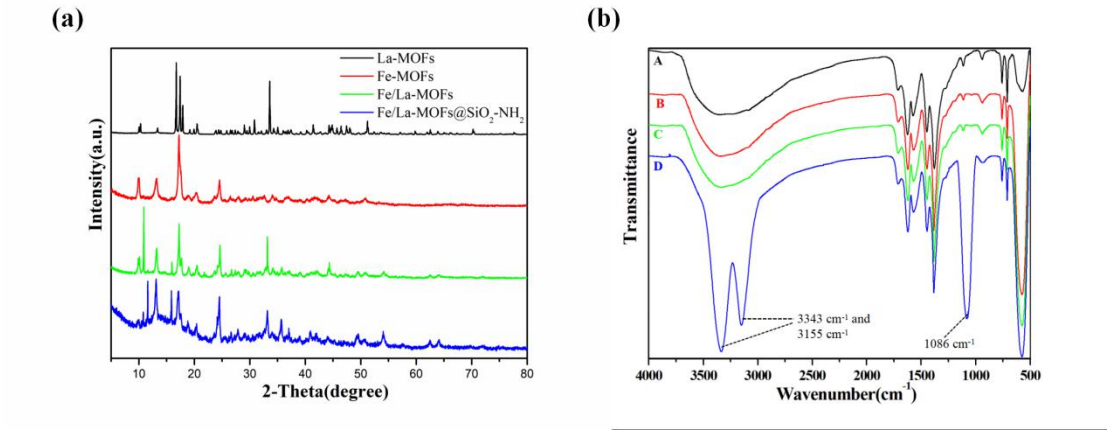


**Figure S4.** XRD patterns and Fourier transform infrared spectroscopy (FT-IR). (a) XRD patterns of La-MOFs, Fe-MOFs,Fe/La-MOFs and Fe/La-MOFs@$SiO_2$-$NH_2$; (b) FT-IR of A: La-MOFs, B: Fe-MOFs, C: Fe/La-MOFs and D: Fe/La-MOFs@$SiO_2$-$NH_2$.

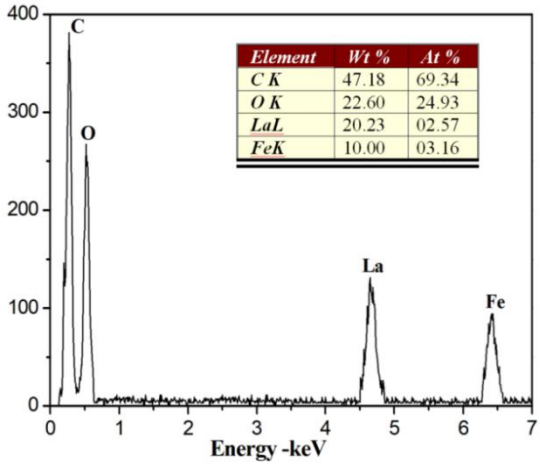


**Figure S5.** Energy dispersive x-ray spectroscopy of the Fe/La-MOFs nanoparticles.

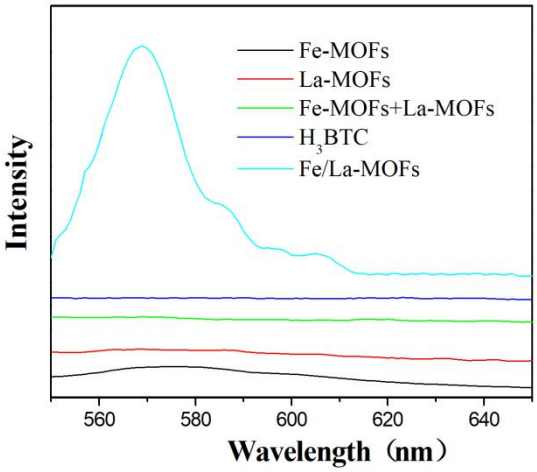


**Figure S6.** Fluorescence spectra of Fe/La-MOFs, La-MOFs, Fe-MOFs, La-MOFs+Fe-MOFs and $H_3BTC$.

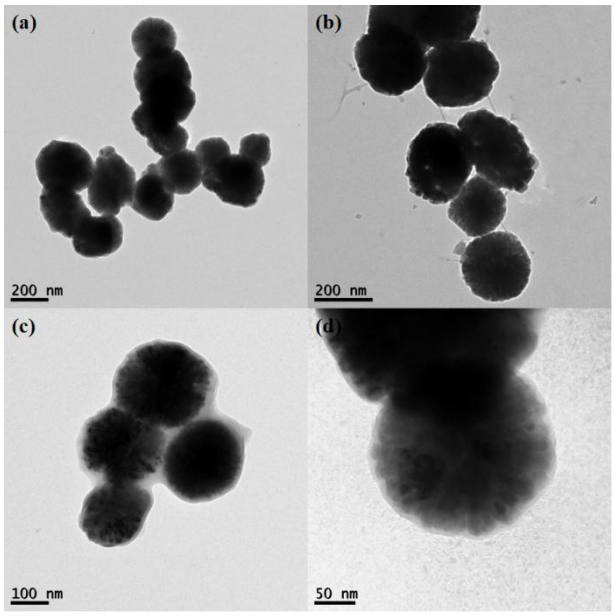


**Figure S7.** (a) and (b) TEM images of Fe/La-MOFs nanoparticles; (c) and (d) TEM images of Fe/La-MOFs@$SiO_2$-$NH_2$ nanoparticles.

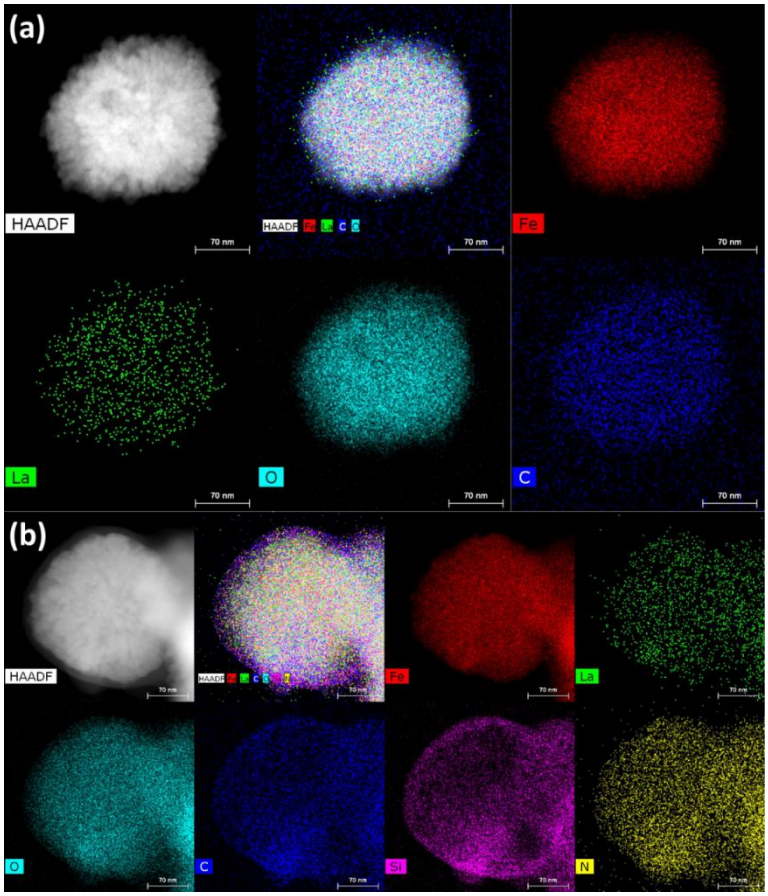


**Figure S8.** EDX elemental mapping and energy dispersive x-ray spectroscopy of (a) the Fe/La-MOFs nanoparticles and (b) the Fe/La-MOFs@$SiO_2$-$NH_2$ nanoparticles.

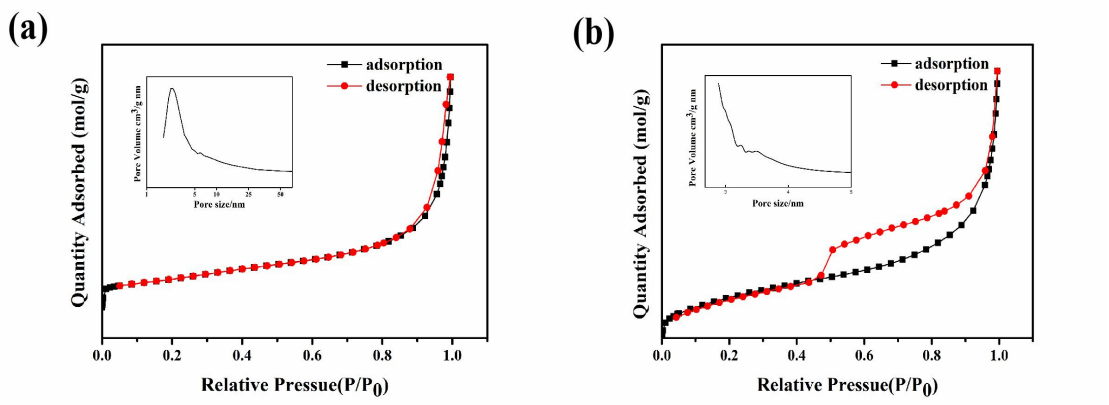


**Figure S9.** Nitrogen adsorption-desorption isotherms and the corresponding pore size distributions of (a) the Fe/La-MOFs and (b) the Fe/La-MOFs@$SiO_2$-$NH_2$ .

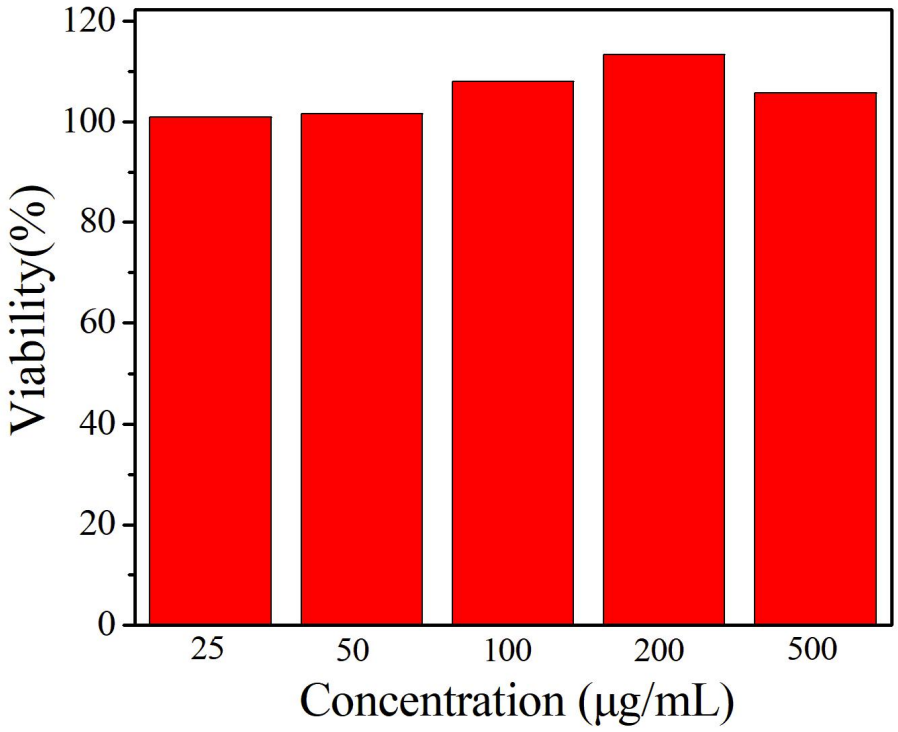


**Figure S10** Cell viability of 4T1 cells exposed to Fe/La-MOFs@$SiO_2$-$NH_2$ at various concentrations.

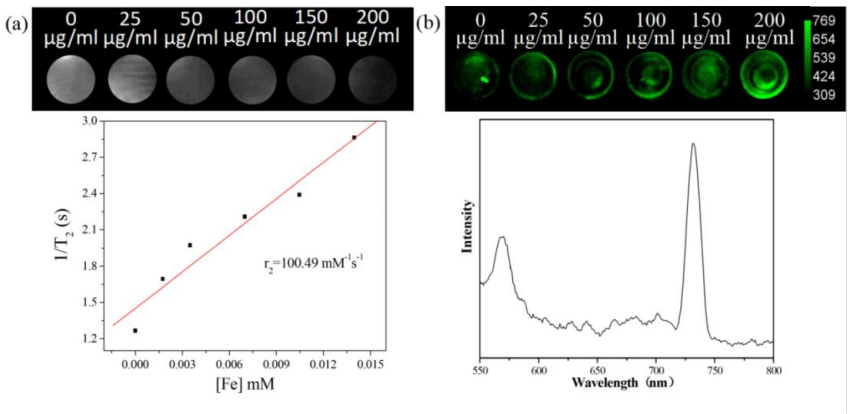


**Figure S11.** (a) $T_2$-weighted MR images and relaxivity plot for aqueous solutions of the Fe/La-MOFs@$SiO_2$-$NH_2$ nanoparticles at 9.4 T; (b) in vitro fluorescence imaging of aqueous solutions of the Fe/La-MOFs@$SiO_2$-$NH_2$ nanoparticles.